Detection and Location of Multiple Wiring Faults via Time–Frequency-Domain Reflectometry

Eunseok Song, *Member, IEEE*, Yong-June Shin, *Member, IEEE*, Philip E. Stone, *Student Member, IEEE*, Jingjiang Wang, *Student Member, IEEE*, Tok-Son Choe, *Member, IEEE*, Jong-Gwan Yook, *Senior Member, IEEE*, and Jin Bae Park, *Senior Member, IEEE*

***Abstract*—In this paper, we propose a high-resolution time–frequency-domain reflectometry technique as a methodology of detection and estimation of faults on a wire. This method adopts the time–frequency cross-correlation characteristics of the observed signal in both the time and frequency domains simultaneously. The accuracy of the proposed method is verified with experiments using a radio-guide-type coaxial cable and comparing it with traditional time-domain as well as frequency-domain reflectometry methods. It is clearly shown here that the proposed algorithm produces excellent results compared to the conventional methods for single as well as multiple fault cables.**

***Index Terms*—Chirp signal, fault detection, fault estimation, time–frequency cross-correlation function, time–frequency-domain reflectometry (TFDR), resolution.**

I. Introduction

SEVERAL aircraft accidents have initiated concerns with the electrical wiring systems of commercial aircraft that exert a great effect on the stability of the whole system [1]. The aging of wires in airplanes and instrument clusters not only lowers the system accuracy but also causes serious problems and faulty operation [2]. Unlike the obvious cracks in a wing or an engine, a damaged wire is extremely difficult to detect. Damaged insulation and the resulting exposed signal conductor could give rise to arcs and shorts, as well as electromagnetic emission and interference, which can be just as deadly. If an external shield or braided internal shield protecting a wire is broken, the resulting wire could radiate or accept electromagnetic energy to an internal component or from the outside. To detect a fault on a transmission line, several techniques are used or are under development based on reflectometry. The state-of-the-art reflectometry methods are mainly categorized by time domain and frequency domain; time-domain reflectometry (TDR) [3] and optical time-domain reflectometry (OTDR) [4] belong to the *TDR* family, while frequency-domain reflectometry (FDR) [5], optical frequency-domain reflectometry (OFDR) [6], and standing-wave reflectometry (SWR) [7] belong to the *FDR* family.

In time-domain approaches, TDR has been traditionally used for locating faults in cables. Currently, high-performance TDR instruments, coupled with add-on analysis tools, are commonly used as the tools of choice for failure analysis and signal integrity characterization of circuit boards, wiring packages, sockets, connectors, and cable interconnects used at gigabit speeds. TDR transmits a very sharp edge waveform down a transmission line to a test device, and then measures the reflections from that device. The measured reflections often make short work of designing signal path interconnects and transmission lines in IC packages, PC board traces, and coaxial cables.

In frequency-domain approaches, SWR involves sending a sinusoidal waveform down the wire, receiving a reflected wave returned from the wire's end, and analyzing the standing wave on the line created from the addition of those two signals. The peaks and nulls of this standing wave give the technician information about the length and terminating load of the cable [7]. A healthy cable's wave pattern will be distinct from that of a cable with an open or short circuit. The advantage that this method has over TDR is that the electronics are simpler, and therefore less expensive. In the cases of both FDR and SWR, resolution depends on the degree of the sweeping frequency [5], [10]. These methods use phase difference to detect fault location. However, FDR exhibits a relatively high error rate due to the phase sensitivity to noise. These methodologies analyze signals in only one domain, and therefore face inherently poor accuracy. The faults in a worn wire could exist as various forms in an actual system, and as a result, conventional methods find it difficult to detect and estimate the characteristics of these faults [5], [10].

However, in practical cases—such as a real trace on a board, which often has to travel through different layers with potentially different impedances, connected with vias and connectors and package mounted on the board—the situation is more complex and we have to deal with an effect known as *multiple reflections*. TDR accurately measures the first discontinuity, but measures each succeeding discontinuity with less accuracy as the transmitted step degrades and multiple reflections occur. The higher resolution of the TDR depends on the shorter rise time of the input pulse. However, shortening the rise time gives rise to a number of aberrations, like preshoot and ringing indications,

Manuscript received January 22, 2006; revised June 27, 2008, September 19, 2006, and October 1, 2008. Current version published February 13, 2009. This work was supported in part by the National Aeronautics and Space Adminstration under Grant NCC5-575, by the Experimental Program to Stimulate Competitive Research (EPSCOR)/South Carolina Research Authority (SCRA) Research Scholarship Program, and by the U.S. Office of Naval Research under Grant N00014-00-0368.

E. Song is with Samsung Electronics, Seoul 100-101, Korea.

Y.-J. Shin, P. E. Stone, and J. Wang are with the Department of Electrical Engineering, University of South Carolina, Columbia, SC 29208 USA (e-mail: shinjune@engr.sc.edu).

T.-S. Choe is with the Agency of Defense Development, Daejon 305-660, Korea, and also with the Department of the Electrical and Electronic Engineering, Yonsei University, Seoul 120-749, Korea.

J.-G. Yook and J. B. Park are with the Department of Electrical and Electronic Engineering, Yonsei University, Seoul 120-749, Korea.

Color versions of one or more of the figures in this paper are available online at http://ieeexplore.ieee.org.

Digital Object Identifier 10.1109/TEMC.2008.2007964

0018-9375/$25.00 © 2009 IEEE

resulting in degraded performance evaluations. The limitation of the sampling rate in TDR instruments themselves is another difficulty for improving resolution. In this paper, we discuss how one can resolve the detection and location of the multiple faults in wirings.

To overcome these difficulties, a smart wiring system needs to be developed for real-time, on-the-spot testing, such as in the event of an in-flight failure. For this purpose, advanced signal-processing-based methodologies have been recently introduced. Noise-domain reflectometry (NDR) [12], spread spectrum time-domain reflectometry (SSTDR), and pseudonoise-domain reflectometry (PNDR) would be examples of the efforts. In this paper, we will utilize time–frequency-domain reflectometry (TFDR) that is characterized by its capability of detecting single as well as *multiple* fault states accurately. The reference signal is designed after careful consideration of the expected measurement accuracy and the frequency response of the wire under test. The proposed TFDR method reveals high accuracy rates by utilizing the time–frequency cross-correlation function. The theoretical foundation of the proposed TFDR algorithm is discussed in Section II and an experimental setup of the reflectometry methodology is described in Section III. In Section IV, the performance of the TFDR and other reflectometry methods are documented for a radio guide (RG) type coaxial cable.

II. Time–Frequency-Domain Reflectometry

In this section, the basic idea of TFDR is discussed. The TFDR algorithm is featured by the design of a reference signal and its cross-correlation function in the time–frequency domain. Time–frequency-domain analysis is also utilized for the detection and location in the radar/sonar systems due to the time-varying spectral characteristics of the scattering signals prevalent in those systems [14], [15]. In this section, we will briefly describe theoretical features of TFDR.

A. Motivations of TFDR From TDR

In order to overcome the problems of TDR, this section starts with the technical challenges of TDR and we will seek a solution via time and frequency localization. Refer to a TDR computer simulation for a single fault located 30 m away in Fig. 1. A fault location can be calculated by

$$d = \frac{\mathrm{VOP} \times t_d}{2} \tag{1}$$

where d is the distance of the fault, VOP is the velocity of propagation of the cable, and t_d indicates the round-trip propagation time of the pulse. The velocity of propagation of a cable in TDR is obtained by a calibration process with a test cable. For this simple case, TDR is able to determine the location of the fault fairly accurately, yet there are problems to consider.

One issue is that the reference signal does not stay at a constant voltage during propagation, but rather it increases with time. This phenomenon is due to the capacitance of the wire under test. The wire itself is acting as a charge capacitor, accumulating voltage over time. This is especially dangerous when considering the fact that if an instrument were to be connected to a wire that had just been subjected to a long

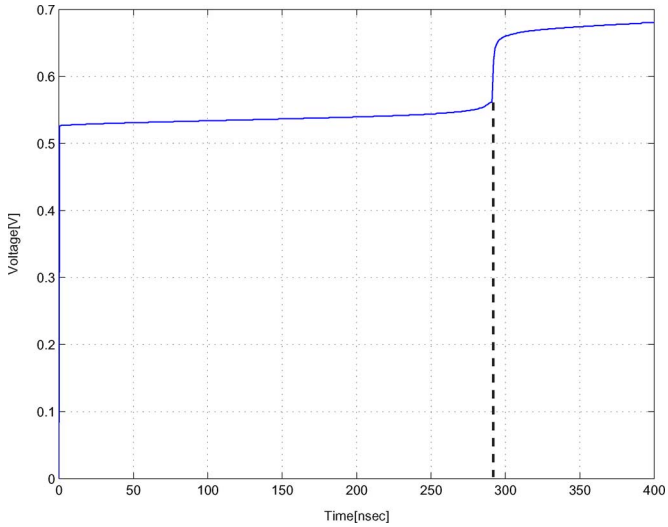

Fig. 1. TDR simulation for the detection and estimation of a fault at 30 m on an RG 142 type coaxial cable (estimated fault location: 30.07 m, error rate: 0.23%).

period of testing and therefore charging, the capacitive wire may discharge into the instrument resulting in costly damage. Also notable is the frequency-dependent attenuation of the signal due to the wire. The ideal step pulse being used in TDR is perfectly localized in the time domain, but is infinite across the frequency domain. Therefore, the frequency-dependent attenuation characteristics of the wire lead to distortion of the ideal step response, as seen in Fig. 1. Rather than a perfectly time-localized response, the response is slower, without a definite rise time. The combination of this voltage charging and the frequency-dependent attenuation on the signal leads to great difficulties in detecting multiple faults. Ideally, TDR would send a step signal down the wire and receive a signal stepped up with twice the magnitude of the transmitted signal for an open fault or stepped back to zero volts for a short. Since the actual transmitted signal is not constant in time, the step pulse is not ideal, the reflected signal is somewhat distorted, and obtaining information for faults after the first one becomes a much greater challenge. Thus, we will utilize time- and frequency-localized reference signals in order to avoid the problems in TDR. The selection and design of reference signals in the time and frequency domains will be discussed in the next section.

B. Resolution in the Time–Frequency Domain

Consider a reference signal $s(t)$ and its time duration and frequency bandwidth. The time duration of the signal σ_t^2 is

$$\sigma_t^2 = \int_{-\infty}^{\infty} (t - \langle t \rangle)^2 |s(t)|^2 \, dt. \tag{2}$$

For convenience of calculation, we assume that $s(t)$ is normalized with time center $\langle t \rangle$. The frequency bandwidth σ_ω^2 can be defined by the Fourier transform of the signal ($S(\omega)$)

$$\sigma_\omega^2 = \int_{-\infty}^{\infty} (\omega - \langle \omega \rangle)^2 |S(\omega)|^2 \, d\omega. \tag{3}$$

The resolution of the TDR is determined by the pulse rise time, which is associated with time duration of the signal (σ_t^2) [8].

Likewise, the resolution of the FDR is determined by the frequency bandwidth of the reference signal (σ_ω^2). Consider the product of the time duration and the frequency bandwidth of the signal, which is typically known as the "uncertainty principle" [8]

$$\sigma_t^2\sigma_\omega^2 = \frac{1}{2}\sqrt{1+4\mathrm{Cov}_{t\omega}^2} \tag{4}$$

$$\geq \frac{1}{2}. \tag{5}$$

The interpretation of the uncertainty principle in terms of signal processing is that there exists a tradeoff between the time duration and the frequency bandwidth of the same signal. The problem is that the reference signal in the time domain localizes information in the time domain with a small time duration σ_t^2; however, its frequency bandwidth σ_ω^2 will increase so that one will lose frequency resolution. Likewise, the reference signal in the frequency domain localizes information in the frequency domain with a small frequency bandwidth σ_ω^2; however, its time duration will increase so that one will lose time resolution.

In order to "optimize" time and frequency resolution together, it is necessary for one to consider time resolution and frequency resolution simultaneously. Referring to the uncertainty principle in (4), the solution of the inequality is obtained by the Gaussian waveform in the time and frequency domains. Therefore, the reference signal in TFDR employs a Gaussian envelope with localized information in both the time and frequency domains. The frequency bandwidth is obtained by examining the frequency characteristics of the test wire and considering the tradeoff between the high fault location resolution at higher frequencies and the more severe attenuation that comes with those higher frequencies. The time duration is typically limited by the minimum rise/fall time of the signal generator being used. The chirp signal envelope functions similarly to the TDR in the time domain, while the linearly modulated sinusoidal signal bears the FDR feature.

The chirp signal $s(t)$ used in this project is as follows:

$$s(t)=\left(\frac{\alpha}{\pi}\right)^{1/4}\exp\left[-\frac{\alpha(t-t_0)^2}{2}+\frac{j\beta(t-t_0)^2}{2}+j\omega_0(t-t_0)\right]. \tag{6}$$

where α, β, t_0, and ω_0 determine the time duration, frequency sweep rate, time center, and frequency center, respectively. Selections of the parameters will be carefully presented in the next section with numerical examples.

C. Time–Frequency Cross-Correlation Function

Without attenuation and distortion of the reflected waveforms, detection and localization would be trivial problems. However, frequency-dependent attenuation of the waveform results in distortions of the reflected waveforms so that it is necessary for one to process the reflected and reference signals for detection and localization purposes. In order to fully explore time and frequency localized properties, it is desirable for us to define a cross-correlation function in both the time and frequency domains.

The time–frequency distribution of the time domain signal used for the detection of a fault in the TFDR system is a Wigner distribution. $W_s(t,\omega)$ is the Wigner distribution of the reference signal and is defined as

$$W_s(t,\omega)=\frac{1}{\pi}\exp\left[-\alpha(t-t_0)^2-\frac{(\omega-\beta(t-t_0)-\omega_0)^2}{\alpha}\right]. \tag{7}$$

The Wigner distribution of the reference and reflected signals aid in evaluation of the time–frequency cross-correlation function. Denote the reflected signal as $r(t)$ and its Wigner distribution as $W_r(t,\omega)$, then one can evaluate a time–frequency cross-correlation function $C_{sr}(t)$ as [9]

$$C_{sr}(t)=\frac{1}{E_sE_r(t)}\times\int_{t'=t-T_s}^{t'=t+T_s}\int_0^{\omega_{\max}}W_r(t',\omega)W_s(t'-t,\omega)\,d\omega\,dt' \tag{8}$$

where $T_s=3\sigma_t$ and $\omega_{\max}$ is the maximum frequency bound. In addition, the normalization of the time–frequency cross correlation $C_{sr}(t)$ is achieved by

$$E_r(t)=\int_{t'=t-T_s}^{t'=t+T_s}\int_0^{\omega_{\max}}W_r(t',\omega)\,d\omega\,dt' \tag{9}$$

$$E_s=\int_{t=-T_s}^{t=T_s}\int_0^{\omega_{\max}}W_s(t,\omega)\,dt\,d\omega. \tag{10}$$

$E_r(t)$ and E_s play a role as normalization factors so that the time–frequency cross-correlation function is bounded between 0 and 1. The difference in time of the peak values in the time–frequency cross-correlation function is converted to fault locations after careful compensation for the frequency-dependent attenuation of the signal due to the media. The values of the time–frequency cross-correlation function above a predetermined threshold value may also be used in the future to estimate the state of faults. It is possible to detect multiple faults in the wiring system with this time–frequency cross-correlation by comparing the similarities of time–frequency information between the reference and the reflected signals. The validity of the aforementioned idea is proven through experimentation with an RG-type coaxial cable in the next section.

III. Experimental Setup

For the detection of multiple faults with the proposed TFDR algorithm, an RG 142 coaxial cable is prepared having two discontinuities caused by possible damage and being open circuited at the end. The term "damage" is used in order to emulate the "soft" incipient faults. The "damage" of the coaxial cable is emulated by a failure of the external shields so that the internal dielectric material is exposed over 1 cm. As shown in Fig. 2, the faults are located at 10 and 20 m from the source. The faulty wire is connected with the TFDR system including a circulator, an arbitrary waveform generator, an oscilloscope, and a control computer, as shown in Fig. 3(a). In addition, a commercial TDR instrument is tested, as shown in Fig. 3(b), for an overall system performance comparison with TFDR.

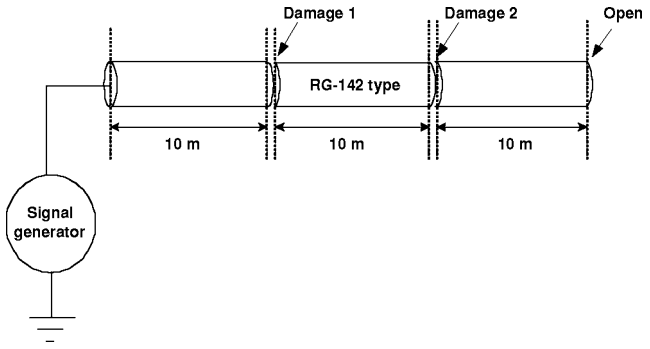

Fig. 2. Diagram of an RG 142 coaxial cable with multiple faults.

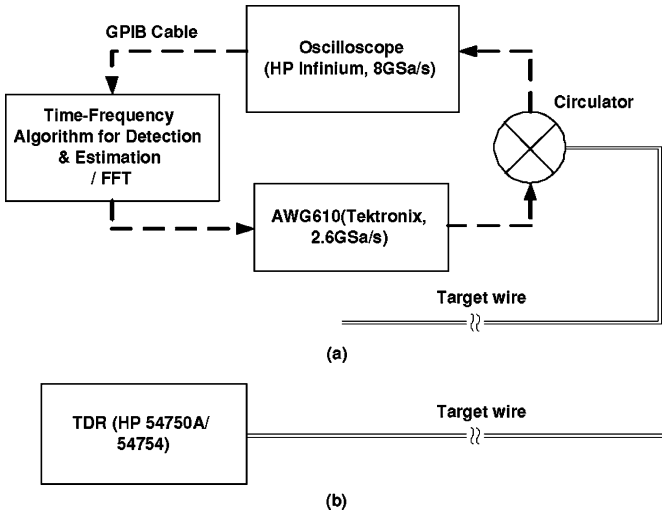

Fig. 3. Experiments setup. (a) TFDR/FDR. (b) TDR.

The TFDR/FDR measurement system consists of an arbitrary waveform generator (Tektronix, AWG610, 2.6 GSa/s) and an oscilloscope (HP Infinium, 8 GSa/s) that are connected to each other with a general-purpose interface bus (GPIB) cable. Using another GPIB cable, the central computer controls these external instruments and executes the time–frequency cross-correlation algorithm with the acquired signal data. The parameters of the reference signal in the time–frequency domain can be chosen via the following process. Let us assign $P_{\rm rec}$ as the received power after the reflection, while $P_{\rm tran}$ is the transmitted power to the cable under test, which is characterized by the attenuation ($\overline{A}$) and length of cable (d). Then

$$P_{\rm rec} = \frac{P_{\rm tran}}{\overline{A}}. \tag{11}$$

In decibel scale calculation

$$[P_{\rm rec}] = [P_{\rm tran}] - [\overline{A}]. \tag{12}$$

For convenience of calculation, normalize the transmitted power, i.e., $[P_{\rm tran}] = 0$. Then

$$\begin{aligned}[P_{\rm rec}] &= -[\overline{A}] \\ &= -[A] \times 2d \end{aligned} \tag{13}$$

where A is attenuation per unit distance. For the proper acquisition of the reflected signal from the cable, the minimum required normalized power is -24 dB. This value is limited by the data acquisition device; the higher the quality of the device, the lower this value can be. Hence

$$[P_{\rm rec}] \geq -24 \text{ dB (minimum required power)}$$
$$-[A] \times 2d \geq -24 \text{ dB}. \tag{14}$$

In this calculation, the length of the cable is chosen to be $d = 40$ m. By choosing a maximum length for calculation that is longer than the cable sample being evaluated, our calculations will be on the safe side. Therefore

$$[A] \leq \frac{24 \text{ dB}}{80 \text{ m}} = \frac{30 \text{ dB}}{100 \text{ m}}. \tag{15}$$

Thus, the reflection signal lower than -24 dB cannot be detected in this experiment. The specifications of the RG 142 cable used for the majority of the simulations and experiments in this paper are given in Table I. The frequency characteristics of this cable are shown in Fig. 4. Referring to Fig. 4, and taking into account the tradeoff between high resolution and amplitude attenuation, a reasonable frequency center can be chosen as

$$f_0 \leq 450 \text{ MHz}. \tag{16}$$

This number is calculated for an RG-type coaxial cable 40 m in length, but the process is valid for any type of cable of any length as long as the attenuation factor per distance A and the length of the cable d are available.

To determine the frequency range of the reference signal, the frequency characteristics of the RG-type coaxial cable shown in Fig. 4 are used. It is observed that the phase characteristics are reasonably well maintained, up to the several hundred

TABLE I
PHYSICAL DIMENSION AND ELECTRICAL PROPERTY PARAMETERS OF THE RG 142 COAXIAL CABLE

Coaxial cable type	Inside radius [mm]	Outside radius [mm]	permittivity (ϵ_r)	loss tangent ($\tan\delta$)
RG-142	0.9398	3.4544	2.1	0.0003

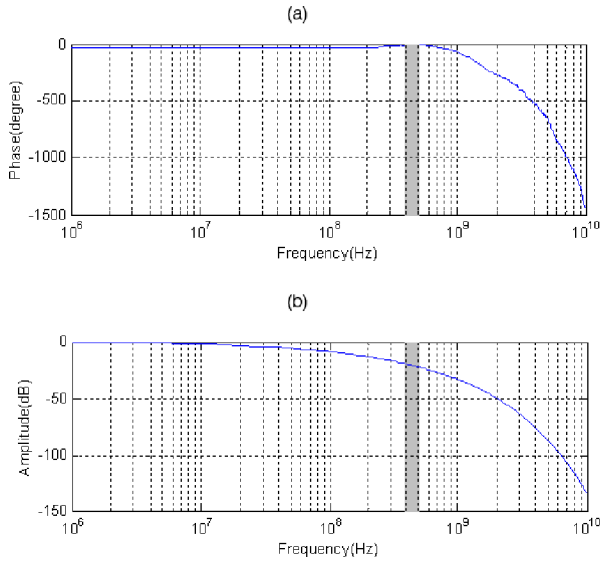

Fig. 4. Characteristics of the RG 142 coaxial cable. (a) Phase response. (b) Amplitude response.

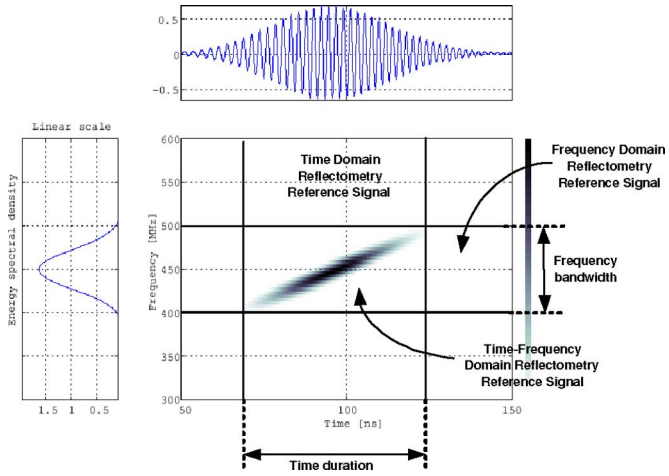

Fig. 5. Comparisons of TDR, FDR, and TFDR on time–frequency distribution of the designed reference signal.

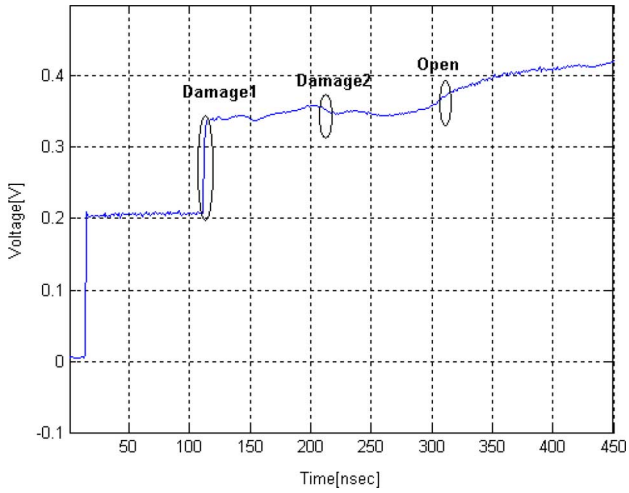

Fig. 6. Waveform of the TDR for a multifault of an RG 142 type coaxial cable.

megahertz region, while the amplitude of the propagating wave rapidly decreases in the gigahertz region. Also, unfortunately, the frequency bandwidth of the chirp signal is limited by the performance of the signal generator and the operating frequency of the circulator that isolates the reflected signal from the fault. Due to the uncertainty principle, the time duration must be factored in as well. A smaller time duration will relate to a smaller dead zone and higher time localization. However, the selected frequency bandwidth influences the determination of the time duration via the uncertainty principle. The time duration is also limited by the minimum rise/fall time of the signal generator and is chosen as 50 ns. A reasonable bandwidth is then chosen as 100 MHz. For an equitable comparison between the FDR and TFDR methods, the FDR frequency range is designated to be 500 MHz, which is identical to the maximum frequency of the TFDR measurement waveform.

The reference input signal for the TDR measurement is a step-pulse function, and that of the FDR is a gigabit-sampled 500-MHz sine wave. The TFDR uses a Gaussian-modulated chirp signal having linearly increasing frequency components (center frequency of 450 MHz, frequency bandwidth equal to 100 MHz, and time duration of 50 ns). In Fig. 5, the designed time–frequency distribution of the reference signal for an RG-type coaxial cable is provided. As shown in the figure, the reference signal provides time localization within 50 ns while the frequency is also localized between 400 and 500 MHz. Note that the Gaussian envelope in the time domain is also reflected in the frequency domain in a scaled manner that allows proper localization simultaneously in both the time and frequency domains at once.

There is a high possibility of multiple faults existing on a real wire system, but many difficulties are accompanied with conventional methods to detect multiple faults. The performance of both conventional and proposed methods will be compared with multiple fault cases. The practical experiment under the described setup will be verified along with the simulation results in a latter section.

IV. Result and Analysis

A. Time-Domain Reflectometry

For comparing the performance of detection and localization of multiple faults, each method (TDR, FDR, and TFDR) has been tested on an RG 142 type coaxial cable. The TDR instrument was used on a cable sample with multiple faults, and the measured waveform can be seen in Fig. 6. Again, a model of the faulty wire being used in the experiment can be seen in Fig. 2 and the experimental setup can be seen in Fig. 3(b). In Fig. 6, the fault at 10 m (damaged) is relatively clear to recognize, but the other faults at 20 m (damaged) and 30 m (open) cannot be identified clearly because of the obscure signal envelope. It is apparent that the distortion caused by the first fault has hindered the ability of the TDR to detect any successive faults. Even with the knowledge of the fault locations, it is difficult for the naked eye to determine at what time the faults occurred and the equipment is also unreliable. Table II shows that even though the multiple faults were all located in simulation, the locations of the second and third faults were unclear using TDR. Thus, it is confirmed that the TDR method has difficulty in detecting multiple faults.

B. Frequency-Domain Reflectometry

FDR sends a sinusoidal signal into a wire/cable and uses the phase difference between that reference signal and the reflected signal due to the fault to estimate the fault location [10]. Fig. 7 depicts the phase difference between a reflected signal from a multiple fault RG 142 coaxial cable and a frequency sweep of reference signal sine waves generated in the AWG610 instrument. The observed phase difference between the reference and reflected signals from a fault at 10 m on an RG 142 type coaxial cable is 174.08°. In the other cases at 20 and 30 m, however, the phase information for the distance cannot be obtained because of an overlap of multiple reflected signals. This phase difference is converted into the distance from the fault after taking the fast Fourier transform (FFT) of the two signals. From the phase

TABLE II
COMPARISON OF THE MULTIFAULT DETECTION AND ESTIMATION RATES AMONG THE TDR, FDR, AND TFDR WITH AN RG 142 COAXIAL CABLE

		Fault location	Detection & Location	Error (m)	Error (%)
TDR	Measured	10m	9.956	0.044	0.44
		20m	N/A	-	-
		30m	N/A	-	-
	Simulated	10m	10.032	0.032	0.32
		20m	20.112	0.112	0.56
		30m	29.842	0.158	0.53
FDR	Measured	10m	11.477	1.477	14.77
		20m	N/A	-	-
		30m	N/A	-	-
	Simulated	10m	8.962	1.038	10.38
		20m	N/A	-	-
		30m	N/A	-	-
TFDR	Measured	10m	9.957	0.043	0.43
		20m	19.938	0.062	0.31
		30m	29.925	0.075	0.25
	Simulated	10m	9.983	0.017	0.17
		20m	19.972	0.028	0.14
		30m	29.818	0.182	0.61

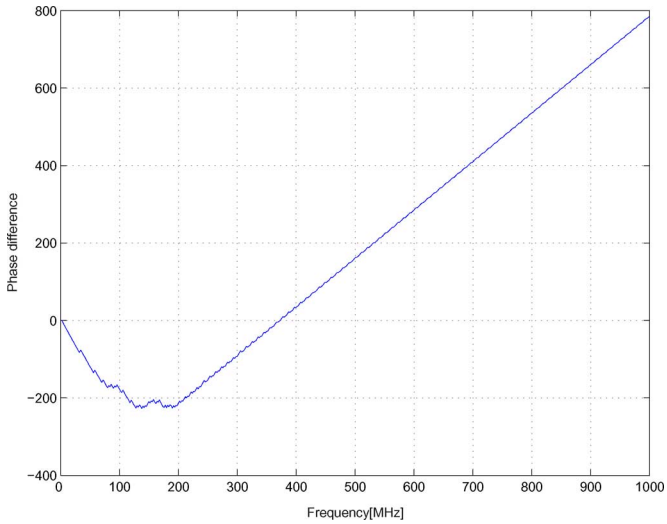

Fig. 7. Phase difference between the reference and reflected signals from a multiple fault RG 142 type coaxial cable.

difference θ_0, the fault location is calculated as follows:

$$d = \frac{\text{VOP} \times \theta_0}{\omega} \tag{17}$$

where d is the distance of the fault, VOP is the velocity of propagation of the cable, and ω is the frequency of the reference signal.

C. Time–Frequency-Domain Reflectometry

Fig. 8(a) shows the time-domain waveform of both the reference and reflected signals generated from the TFDR measurement, and Fig. 8(b) shows the time–frequency cross-correlation results. The results of the former methods clearly reveal the difficulty in locating the reflected signals due to the attenuation and multiple reflections. However, the TFDR method reveals that the time–frequency cross-correlation captures even a small signature in time-domain data. Moreover, the time–frequency cross-correlation function can detect multiple faults along the cable.

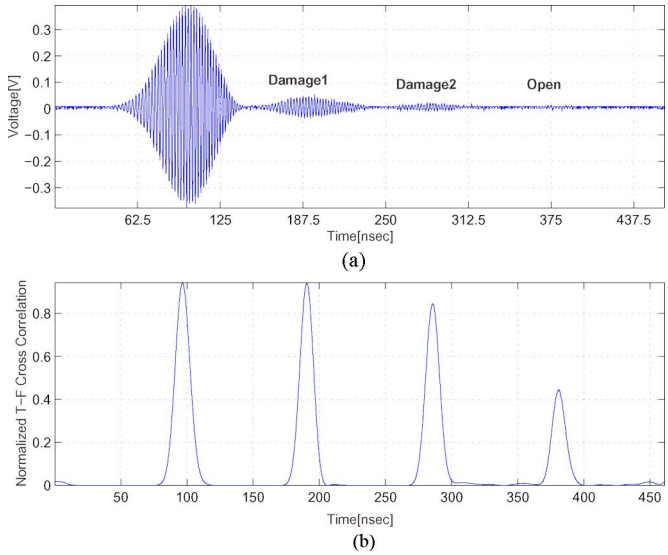

Fig. 8. (a) Time series of the reference and reflected signals. (b) Time–frequency cross-correlation graph for multiple faults in an RG 142 coaxial cable.

Table II summarizes the results of the simulations and experiments with the TDR, FDR, and TFDR. The errors in the TDR and TFDR methods converge within a reliability range of 1% to the nearest fault. However, the error of the FDR exceeds 10% due to high sensitivity to noise and a lack of error compensation. This vulnerability to noise is a major drawback of the FDR method.

For the multiple fault case, the theoretical TDR and TFDR results for each fault location have an error rate of less than 1%, whereas the FDR simulation was unable to collect data for more than one fault. However, neither the TDR nor FDR methods could physically detect signals from the second and third discontinuities. Yet, the proposed TFDR algorithm produces very accurate measurement results for both the first fault and the multiple faults thereafter. The error rate is less than 0.5% at each fault location for each type of fault. It is clear from these measurements that TFDR presents higher accuracy and greater robustness to noise than the other methods.

Again, this is due to the fact that the TFDR reference signal is a Gaussian waveform localized in both the time and frequency domains rather than just one or the other. The time duration and frequency bandwidth of the signal allow it to adhere to the uncertainty principle and provide sufficient resolution in both time and frequency. TFDR also has the ability to detect and locate multiple faults within a reliable error rate whereas the other methods were unreliable after a single fault. This proves that TFDR can be a sufficient and superior method for fault detection and localization in real-world environments.

V. MULTIPLE REFLECTION

The experimental results and comparisons of TDR, FDR, and TFDR discussed in previous sections are promising. But if we consider a lattice diagram of reflection, the experimental setup in Fig. 3 may cause constructive reflections as the faults are evenly located on the wire. Thus, in order to adequately demonstrate

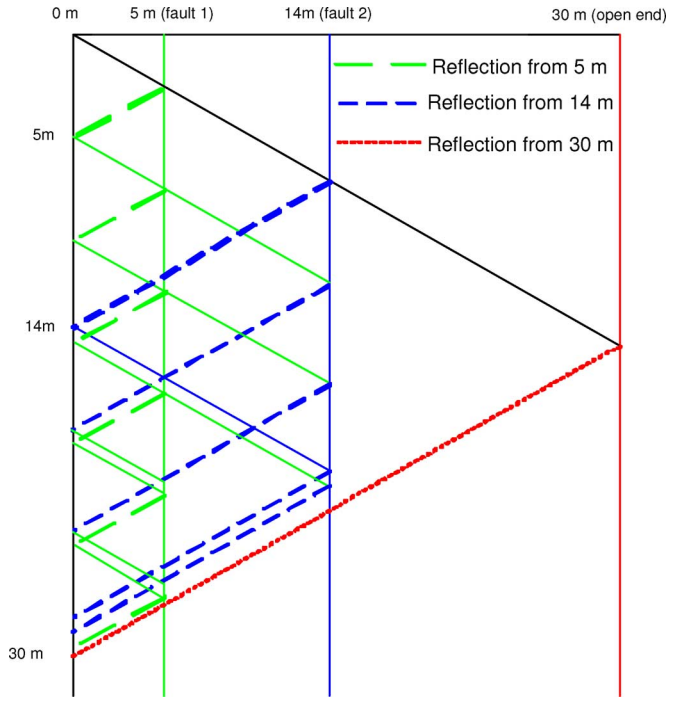

Fig. 9. Lattice diagram of the multiple reflections from 5, 14, and 30 m.

the strengths of the joint time–frequency-domain reflectometry (JTFDR) technique, it is necessary to provide results for a situation where the fault separations are significantly different so that the intermediate waves, due to secondary reflections, will be clearly visible.

Considering the Bewely lattice diagram, we carried out another experiment on multiple fault detection and location via TFDR. In order to clarify the issues of the multiple reflections, we used a 30-m-long RG 58 coaxial cable that has defects located at 5 and 14 m so that we can avoid the problem of the constructive reflections. In Fig. 9, the experimental fault settings are provided with the corresponding Bewely lattice diagram, which confirms the fact that the locations of the defects would not generate significant interference at 5 and 14 m.

In Fig. 10, the waveforms used for detection and location of multiple faults via TFDR are provided. The transmitted and reflected waves in the time domain are provided in Fig. 10(a) (top) and its time–frequency cross-correlation function is provided in Fig. 10(b) (bottom). The first defect located at 5 m and the second defect located at 14 m are detected and located. The value of the time–frequency cross-correlation function of the defect at 14 m is less than that of the defect located at 5 m, but it is above the normalized threshold value of 0.1 for detection and location. Also, this result can be interpreted with the lattice diagram provided in Fig. 9.

As shown in Fig. 10, TFDR can accurately detect and locate the faults at 5 and 14 m. In addition, the open termination of the cable located at 30 m is clearly identified by the time–frequency cross-correlation function. Theoretically, the multiple reflections still interact but the contribution for detection and location of TFDR is almost negligible in this experiment. This example shows that the detection and location of multiple faults

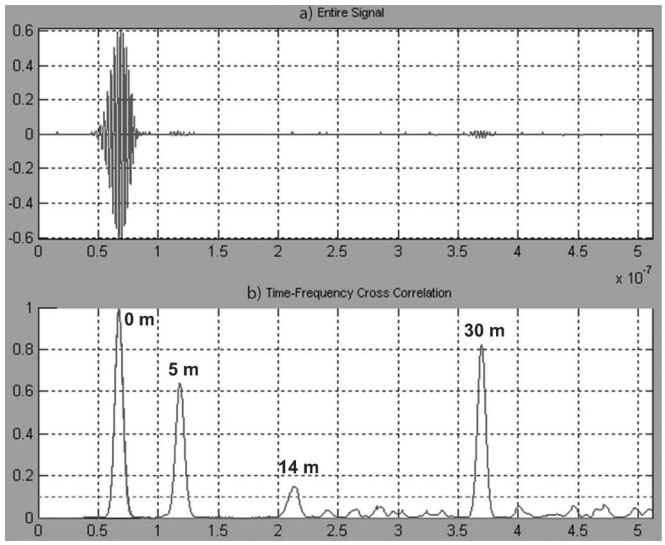

Fig. 10. (a) Time series of the reference and reflected signals. (b) Time–frequency cross-correlation graph for multiple faults in an RG 58 coaxial cable.

described in the paper is not because of constructive reflection from other faults, but TFDR does detect and locate the "real" reflections from the faults. But, as shown in Fig. 10, the accuracy and sensitivity of detection decrease as the multiple faults' distance increases. This result is due to the attenuation of the reflected signal, which is not avoidable in the coaxial cable. However, this research exhibits a technical advantage of the proposed reflectometry technique to detect and locate multiple faults by use of simultaneous time- and frequency-domain analyses.

VI. Conclusion

Based on the time–frequency cross-correlation analysis of the chirp signal, the extremely accurate TFDR method is proposed and validated with considerable measurements and verified results. With the TFDR algorithm, both the experimental and simulated results show an error rate of less than 1.0% for all cases, which is much less than the TDR and FDR results. Furthermore, the proposed method is able to detect and estimate single as well as multiple faults along a wire, while the traditional methods systematically reveal their limitations. Therefore, it can be concluded that TFDR is an excellent reflectometry method with higher resolution in detection and estimation results, even considering multiple faults and various fault types. This TFDR is also expected to be useful in other areas of study such as impedance testing in signal integrity. The time–frequency cross-correlation function will also allow us to measure the reflected energy from faults. Along with this information, the phase differences between the reference and reflected signals may indicate the impedance of the faults. Clearly, TFDR has the potential to be a more accurate means of fault detection and location than the current state-of-the-art technology and has the potential to make an impact in even more aspects of engineering.

References

[1] C. Furse and R. Haupt, "Down to the wire: The hidden hazard of aging aircraft wiring," *IEEE Spectr.*, vol. 38, no. 2, pp. 35–39, Feb. 2001.

[2] C. Teal and C. Satterlee, "Managed aircraft wiring health directly relates to improved avionics performance," in *Proc. Digit. Avionics Syst. Conf.*, 2000, vol. 1, pp. 3B6-1–3B6-6.
[3] S. Navaneethan, J. J. Soraghan, W. H. Siew, F. McPherson, and P. F. Gale, "Automatic fault location for underground low voltage distribution networks," *IEEE Trans. Power Del.*, vol. 16, no. 2, pp. 346–351, Apr. 2001.
[4] A. Beghi and M. Bertocco, "A robust fault detection algorithm for the improvement of OTDR sensitivity," in *Proc. IEEE Instrum. Meas. Technol. Conf. (IMTC 1996) Quality Meas.: Indispensable Bridge Between Theory Reality*, vol. 2, pp. 818–821.
[5] H. Vanhamme, "High resolution frequency-domain reflectometry," *IEEE Trans. Instrum. Meas.*, vol. 39, no. 2, pp. 369–375, Apr. 1990.
[6] M. Wegmuller, M. Legre, P. Oberson, O. Guinnard, L. Guinnard, C. Vinegoni, and N. Gisin, "Analysis of the polarization evolution in a ribbon cable using high-resolution coherent OFDR," *IEEE Photon. Technol. Lett.*, vol. 13, no. 2, pp. 145–147, Feb. 2001.
[7] N. Kamdor and C. Furse, "An inexpensive distance measuring system for location of robotic vehicles," in *Proc. IEEE Int. Symp. Antennas Propag. Soc.*, 1999, vol. 3, pp. 1498–1501.
[8] L. Cohen, "Time-frequency distributions—A review," *Proc. IEEE*, vol. 77, no. 7, pp. 941–981, Jul. 1989.
[9] Y. J. Shin, E. S. Song, J. W. Kim, J. B. Park, J. G. Yook, and E. J. Powers, "Time-frequency domain reflectometry for smart wiring systems," in *Proc. SPIE's 47th Int. Symp. Optacal Sci. Technol.*, Jul. 2002, vol. 4791, pp. 86–95.
[10] C. Furse, Y. C. Chung, R. Dangol, M. Nielsen, G. Mabey, and R. Woodward, "Frequency-domain reflectometry for on-board testing of aging aircraft wiring," *IEEE Trans. Electromagn. Compat.*, vol. 45, no. 2, pp. 306–315, May 2003.
[11] Y. C. Chung, C. Furse, and J. Pruitt, "Application of phase detection frequency domain reflectometry for locating faults in an F-18 flight control harness," *IEEE Trans. Electromagn. Compat.*, vol. 47, no. 2, pp. 327–334, May 2005.
[12] C. Lo and C. Furse, "Noise-domain reflectometry for locating wiring faults," *IEEE Trans. Electromagn. Compat.*, vol. 47, no. 1, pp. 97–104, Feb. 2005.
[13] Y.-J. Shin, T. Choe, E. Song, J. Park, J. Yook, and E. J. Powers, "Application of time-frequency domain reflectometry for detection and localization of a fault on a coaxial cable," *IEEE Trans. Instrum. Meas.*, vol. 54, no. 6, pp. 2493–2500, Dec. 2005.
[14] V. C. Chen and H. Ling, "Joint time-frequency analysis for radar signal and image processing," *IEEE Signal Process. Mag.*, vol. 16, no. 2, pp. 81–93, Mar. 1999.
[15] B. Boashash, *Time-Frequency Methods in Radar, Sonar & Acoustics, Time-Frequency Signal Analysis and Processing: A Comprehensive Reference*. Oxford, UK: Elsevier, 2003, ch. 14, pp. 577–625.

Eunseok Song (S'01–M'03) received the B.S degree in electronic engineering from Hongik University, Seoul, Korea, in 2001, and the M.S. degree in electrical and electronic engineering from Yonsei University, Seoul, in 2003.

Since 2003, he has been with Samsung Electronics, Seoul, where he is involved in the design and modeling of high-speed package interconnects, power distribution networks, EMI/EMC analysis for system-in-package and chip-package-board coanalysis.

Yong-June Shin (S'99–M'04) received the B.S. degree (with early completion honors) from Yonsei University, Seoul, Korea, in 1996, the M.S. degree from the University of Michigan, Ann Arbor, in 1997, and the Ph.D. degree from The University of Texas at Austin, Austin, in 2004.

He joined the Department of Electrical Engineering, University of South Carolina, Columbia, as an Assistant Professor. His current research interests include power engineering/power electronics, with emphasis on power quality and harmonics, and advanced signal processing theory: time–frequency analysis, wavelets, and higher order statistical signal processing.

Dr. Shin is the recipient of the National Science Foundation CAREER Award in 2008 and GE Korean–American Education Commission Scholarship.

Philip E. Stone (S'05) received the B.S. degree in electrical engineering in 2005 from the University of South Carolina, Columbia, where he is currently working toward the Ph.D. degree in the Department of Electrical Engineering.

His research interests include time–frequency analysis, power quality, power systems and electronics, and digital signal processing.

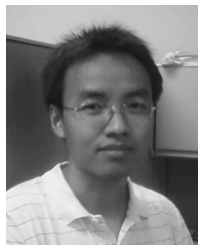

Jingjiang Wang (S'05) received the B.S and M.S. degrees from the HuaZhong University of Science and Technology, Wuhan, China, in 2000 and 2003, respectively. He is currently working toward the Ph.D. degree in the Department of Electrical Engineering, University of South Carolina, Columbia.

His research interests include time–frequency analysis, power quality, power systems and electronics, and digital signal processing.

Tok-Son Choe (M'04) received the B.S. degree in 2003 from Yonsei University, Seoul, Korea, where he is currently working toward the M.S. degree in the Department of the Electrical and Electronic Engineering.

He is with the Agency of Defense Development, Daejon, Korea. His research interests include time–frequency analysis, wavelet, communication systems, and robotics.

Jong-Gwan Yook (S'89–M'02–SM'04) received the B.S. and M.S. degrees from Yonsei University, Seoul, Korea, in 1987 and 1989, respectively, and the Ph.D. degree from the University of Michigan, Ann Arbor, in 1996, all in electrical engineering.

From 1998 to 1999, he was a Senior Engineer at Qualcomm, Inc., San Diego, CA. From 1999 to 2000, he was an Assistant Professor at the Kwang-Joo Institute of Science and Technology. He is currently an Associate Professor in the Department of Electrical and Electronic Engineering, Yonsei University, where he is also the Director of the Advanced Computational Electromagnetics Laboratory. His research interests include microwave circuits and antennas, RF microelectromechanical systems, computational electromagnetics, EMI/EMC analysis as well as high-speed digital design and packaging.

Jin Bae Park (SM'04) received the B.S. degree from Yonsei University, Seoul, Korea, in 1977, and the M.S and Ph.D. degrees from Kansas State University, Manhattan, in 1985 and 1990, respectively, all in electrical engineering.

From 1990 to 1991, he was an Assistant Professor in the Department of Electrical and Computer Engineering, Kansas State University. Since 1992, he has been a Professor in the Department of Electrical and Electronic Engineering, Yonsei University, where he is also the Director of the Control Engineering Laboratory and Automation Technology Research Center. His current research interests include measurement and instrumentation, optics, nonlinear control, robust control, fuzzy systems, neural networks, signal processing, and robotics.